Photoluminescence characteristics of heavily Ho^{3+}-doped BaY_2F_8 and CaF_2 crystals

Taiju TSUBOI[1]
Silviu POLOSAN[1,2]
Kiyoshi SHIMAMURA[3]
Hyo-Jin SEO[4]
[1] Faculty of Engineering, Kyoto Sangyo University, Kyoto 603-8555, Japan
[2] National Institute of Materials Physics, Bucharest-Magurele, PO Box MG-7, 077125, Romania
[3] Optronic Materials Center, National Institute for Materials Science, Tsukuba 305-0044, Japan
[4] Department of Physics, Pukyong National University, Busan 608-737, Republic of Korea

1. Introduction

Holmium-doped crystals play an important role in practical applications including medicine and eye-safe remote sensing system, coherent Doppler velocimetry and gas detection [1], because Ho^{3+} ions doped in insulating crystals give strong emission at near infrared 1.9-2.1 μm [2, 3, 4]. This emission is caused by electronic transition $^5I_7 \rightarrow {}^5I_8$ in Ho^{3+} ion. This Ho^{3+} infrared emission has been confirmed to give laser action in various host crystals since early work with $YLiF_4$ crystal [5, 6]. The spectral region around 2 μm is absorbed by liquid water, therefore Ho-laser is used as eye-safe laser in medical treatment for patients with superficial bladder carcinoma [2] and for eye posterior segment surgery [7]. The Ho-laser is also useful for laser radar imaging because the light around 2 μm shows high atmospheric transmittance and low back-ground noise.

High performance of the near-infrared Ho^{3+} laser action is requested for the practical applications. Intense photoluminescence (PL) from Ho^{3+} is necessary to achieve the high performance. To enhance the PL intensity, change of host crystal, change of pumping source including the excitation wavelength, and increase of concentration of Ho^{3+} ions doped in host crystal are conceivable. Most PL studies have been made for crystals with the relatively low concentrations around 0.5-5.0 % Ho^{3+} ions to avoid concentration quenching.

The present work was undertaken to investigate the characteristics of infrared emission bands of heavily Ho^{3+}-doped crystals, together with visible Ho^{3+} emission bands. Here we investi-

gate the PL spectra of (1) monoclinic-structure crystals of BaY_2F_8 doped with 10 and 35 % Ho^{3+} ions and (2) cubic-structure crystal of CaF_2 doped with 30 % Ho^{3+} ions, in a wide spectral region of visible and near infrared, and compare them with those of lightly doped crystals.

2. Experimental procedure

Single crystals of heavily Ho^{3+}-doped BaY_2F_8 and CaF_2 were grown by the following method. Crystal growth was carried out in a CZ system with a 30 kW R.F. generator. High purity powders (>99.99%) of commercially available BaF_2, YF_3, CaF_2 and HoF_3 were utilized. BaF_2 and YF_3 were weighted and mixed in stoichiometric composition. Purification of the raw materials was carried out in a Pt/graphite crucible, heating at 700 C for a period of 12 hours under vacuum (approx. 10^{-3} Pa). This vacuum level, obtained by a rotary and a diffusion pump, was necessary to eliminate effectively the water and oxygen present in the chamber and raw materials, since such a contamination is well-known to be very detrimental for the optical quality of fluoride crystals. Subsequently high purity CF_4 gas (99.99%) was slowly flowed into the furnace, and then the powders were melted. After seeding, crystal rotation and pulling rates were fixed at 10 rpm and 1 mm/h, respectively.

Two crystals of BaY_2F_8 doped with 10 and 35 % Ho^{3+} ions were grown, while a crystal of CaF_2 doped with 30 % Ho^{3+} ions was grown. For comparison with these heavily doped crystals, we measured the photoluminescence spectra of lightly (1 mol %) Ho^{3+}-doped YVO_4 crystal. This crystal was supplied from Prof. M. Bettinelli of Verona University.

Absorption spectra were measured with a Shimadzu UV-3100 spectrophotometer at room temperature. Photoluminescence spectra were measured with a Horiba Spex Fluorolog-3 spectrophotometer at room temperature and 12 K. Infrared spectra were measured in a spectral range between 800 to 2500 nm using a liquid-nitrogen cooled Jobin-Yvon DSSX-IGA010L InGaAs photodiode. Light from a 450 W Xenon lamp was used to excite the crystals.

3. Experimental results and discussion

3.1 Absorption and PL spectra

Figures 1 and 2 show absorption spectra of Ho^{3+}-doped BaY_2F_8 and CaF_2 crystals in ultraviolet-visible and near infrared ranges at room temperature, respectively. These crystals are transparent in 190-3100 nm spectral range. Sharp absorption bands due to Ho^{3+} appear at ultraviolet-visible-infrared range between 242 and 2100 nm. All the bands agree with the Dieke energy level dia-

gram of trivalent Ho^{3+} $(4f)^{10}$ ion [8]. For example, absorption bands due to the $^5I_8 \rightarrow {}^3K_7$ and $^5G_4$ transitions are observed at 386 and 392 nm, respectively. Of many Ho^{3+} absorption bands appeared in the visible spectral range, absorption band at 745-770 nm due to the $^5I_8 \rightarrow {}^5I_4$ transition is the weakest. Three infrared absorption bands appear at 880-920, 1135-1205, and 1850-2095 nm, which are due to the $^5I_8 \rightarrow {}^5I_5$, $^5I_8 \rightarrow {}^5I_6$, and $^5I_8 \rightarrow {}^5I_7$, respectively (Fig. 3). Each absorption band in these visible and infrared bands consists of several separated sharp lines in BaY_2F_8, while each band consists of a few homogeneous broad bands in CaF_2, indicating that Ho^{3+} ions have various site symmetries. This is consistent with the result of selective laser excitation for Ho^{3+}-doped CaF_2 crystals [9]. Two sites are found for Ho^{3+} ions. These sites have been suggested to be the tetragonal and trigonal sites. In addition to these two sites for the isolated Ho^{3+} ions, a family of similar sites are found to be dimers and/or higher-order clusters [9].

Figure 4 shows the PL spectrum of 10% Ho^{3+}-doped BaY_2F_8 crystal which was excited at 285 nm at room temperature. All the emission bands locate at almost the same wavelengths as the absorption bands. The PL excitation spectrum (PLE spectrum) for 660 nm emission is shown in Fig. 5. This PLE spectrum is similar to the absorption spectrum. Figure 6 shows the PL spectrum of Ho^{3+}-doped CaF_2 crystal which was excited at 383 nm at 12 K. Intense emission band is observed at about 660 nm, while the emission band at about 550 nm is very weak.

Characteristics of broad and structure-less absorption bands observed in CaF_2 are reflected in the PL bands, while relatively and sharp emission bands are observed in BaY_2F_8, as seen in Figs. 7-10. Figure 7 shows PL spectra of Ho^{3+}-doped BaY_2F_8 and CaF_2 crystals in visible range at room temperature, while Fig. 4 shows PL spectra at 12 K. It is noted that 550 nm emission due to $^5S_2 \rightarrow {}^5I_8$ transition is considerably weaker than the other emission bands, especially it is negligible in CaF_2 at room temperature (Fig. 7). The 550 nm emission is still weak in BaY_2F_8 even at low temperature such as 12 K. The 550 nm emission in CaF_2 can be observed in CaF_2 as shown in enlarged spectrum of curve 3 in Fig. 8. This is quite different from lightly doped crystal such as YVO_4 doped with 1% Ho^{3+} ions (see Fig. 8) [4]. It is estimated that ratio of the 550nm PL intensity to the 660nm PL intensity is 0.0012, 0.0443, and 12.72 in 35% Ho^{3+}-doped CaF_2, 30% Ho^{3+}-doped BaY_2F_8, and 1% Ho^{3+}-doped YVO_4, respectively, which were excited at 455 nm at 12 K. The 1% Ho^{3+}-doped YVO_4 exhibits intense $^5I_4 \rightarrow {}^5I_8$ emission at 750 nm, the intensity ratio of the 550 nm emission to the 750 nm emission is about 3.25. The 750 nm emission is not observed clearly in both the heavily doped BaY_2F_8 and CaF_2 crystals.

Emission at around 750 nm has been attributed to the transition $^5S_2 \rightarrow {}^5I_7$ in Ho^{3+}-doped in BaY_2F_8 [10] and in Ho^{3+}-doped in $LiTaO_3$ [11]. The emission band has a peak at 750.0 nm in our Ho^{3+}-doped in BaY_2F_8 crystal, and absorption due to the $^5I_8 \rightarrow {}^5I_4$ transition has a peak at 750.0 nm.

Therefore it is reasonable to assign the 750 nm emission to its reverse transition $^5I_4 \rightarrow {}^5I_8$.

Figure 9 shows the PL spectra of heavily Ho^{3+}-doped BaY_2F_8 and CaF_2 crystals in near infrared range at room temperature, while Fig. 10 shows the PL spectra of not only the heavily doped crystals but also lightly Ho-doped YVO_4 at 12 K. Much intense emission is observed around 2100 nm at both temperatures, while an emission band around 890 nm is much weaker than another less-intense emission band around 1200 nm. It is estimated that ratio of the 1200nm PL intensity to the 2100nm PL intensity is 0.042, 0.22, 0.045, and 0.01 in 35% Ho^{3+}-doped CaF_2, 10% Ho^{3+}-doped BaY_2F_8, 30% Ho^{3+}-doped BaY_2F_8, and 1% Ho^{3+}-doped YVO_4, respectively, which were excited at 447 nm at 15 K. When excited at 533 nm, almost the same infrared PL spectra are observed as shown in Figs. 11 and 12.

Figure 13 shows the excitation spectra for 2100 nm emission in Ho^{3+}-doped CaF_2 and BaY_2F_8 crystals at room temperature. These PLE spectra are almost similar to the absorption spectra, indicating that the 2100 nm emission is generated by excitation into all the excited states corresponding to the absorption bands at 300-670nm. The same excitation spectra were obtained for the other infrared emissions at room temperature and 12 K (Figs. 14 and 15). It is noted that, unlike the case of the excitation for the infrared emission, the 660nm emission is not efficiently generated in CaF_2 by excitations at 420 and 540 nm that correspond to the excitation into the $^5G_5$ and $^5S_2$ states, respectively.

Four Ho^{3+} absorption bands appear at 745-770, 880-920, 1135-1205, and 1850-2095 nm in a spectral range of 700-2400 nm in BaY_2F_8 and CaF_2 crystals. The absorption band intensity increases on going from short wavelength to long wavelength, i.e., the 745-770 nm band is the weakest, while the 1850-2095 nm band is the biggest (Figs. 1 and 2). The 745-770, 880-920, 1135-1205, and 1850-2095 nm bands are caused by the $^5I_8 \rightarrow {}^5I_n$ (n=4, 5, 6 and 7) transitions, respectively, which are the same L-L (L: orbital angular quantum number) state transitions in the same spin state S=2 (S: spin quantum number). Only different is the total angular quantum state J. From the Laporte selection rule for the J state, $\Delta J=0, 1$ is allowed, and the transition probability decreases as deviation from $\Delta J=0, 1$ becomes large. The selection rule is rather strongly applicable for transition of $\Delta J=4$ [12]. This means that only the $^5I_8 \rightarrow {}^5I_7$ transition is allowed, the $^5I_8 \rightarrow {}^5I_6$ transition is partially allowed, the $^5I_8 \rightarrow {}^5I_5$ transition is a slightly allowed, and the $^5I_8 \rightarrow {}^5I_4$ transition is forbidden. Therefore it is understood the reason why the 1850-2095, 1135-1205, 880-920, 745-770 nm bands are observed to have the biggest, second biggest, third biggest intensity, and the weakest intensity, respectively.

In addition to the 1135-1205 and 1850-2095 nm emission bands, very weak and sharp emission bands are observed at 977 and 1475nm in 35% Ho^{3+}-doped CaF_2 and 30% Ho^{3+}-doped BaY_2F_8 crys-

tals, but not in 10% Ho^{3+}-doped BaY_2F_8 crystal as shown in Fig.16. These 977 and 1475 nm emissions are generated by excitation at 359, 450, 481 and 645 nm, but not generated by excitation at 535 nm (which corresponds to the excitation into the $^5S_2$ state of single ion of Ho^{3+}). There are no corresponding energy levels in Ho^{3+} to assign the 977 and 1475 nm emissions. Therefore, taking into account that these emissions are observed in heavily doped crystals, it is suggested that they are attributed to Ho^{3+}-pair or cluster. This is consistent with the observation of emission band due to Ho^{3+}-pair at around 1000 nm in Ho^{3+}-doped CaF_2 [9].

3.2 Temperature dependence of PL spectra

Figure 17 shows the near infrared PL spectra of 35% Ho-doped CaF_2 at various temperatures between 270 K and 12 K, which was excited at 360 nm. Two emission bands with peaks at 2110 nm and 1210 nm at room temperature increase the intensities and shift to high energy (at 2032 nm and 1192 nm at 12 K, respectively) with increasing temperature. The enlarged spectra of these 2040 and 1190 nm bands are shown in Figs. 22 and 23, respectively. The 2040 nm band consists of three sub-bands with peaks at about 2105 nm (4750 cm^{-1}), 2040 nm (4902 cm^{-1}), and 1980 nm (5050 cm^{-1}) at 12 K. The 1190 nm band also consists of three sub-bands with peaks at about 1210 nm (8260 cm^{-1}), 1190 nm (8403 cm^{-1}), and 1170 nm (8550 cm^{-1}). The middle sub-band enhances largely and shifts to high energy with decreasing temperature in the both bands. Figures 18 and 19 are drawn in the wavenumber linear scale and in the same range of 1000 cm^{-1}. It is found that the spectral line shapes of the two 2040 and 1190 nm bands are quite similar to each other. Figure 20 plots the peak heights of the two emission bands against temperature, which were measured from the highest peak height each of the two bands. The two bands also show the same behavior in the temperature dependence of the peak intensity.

Figure 21 shows the temperature dependence of the PL spectra of 35% Ho-doped CaF_2 in the visible spectra range, which was excited at 360 nm. Like the case of the near-infrared bands, two emission bands at 658 and 493 nm increase the intensities with increasing temperature. The enlarged spectra of these 658 and 493 nm bands are shown in Figs. 22 and 23, respectively. They are drawn in the wavenumber linear scale and in the same range of 1000 cm^{-1}. The 493 nm band consists of three sub-bands at 12 K, while the 658 nm band consists of four sub-bands. From the four enlarged figures, it is found that the 2040, 1190 and 493 nm band line shapes are quite similar to each other. This indicates that these three emission band shapes reflect the energy levels of the common ground state $^5I_8$, while the 658 nm band shape reflects partially the energy level of its excited state $^5F_5$.

Acknowledgement

The present work was supported by Joint Research Project under the Korea-Japan Basic Cooperation Program which was established by Korea Science and Engineering Foundation (KOSEF) and the Japan Society for Promotion of Science (JSPS).

References:

[1] V. Sudesh, K. Asai, K. Shimamura, T. Fukuda, IEEE J. Quantum Electron. 38 (2002) 1102.

[2] H. Johnson, Lasers in Surgery and Medicine 14 (1994) 213.

[3] M. Schellom, A. Hirth, C. Kieleck, Opt. Lett., 28 (2003) 1933.

[4] S. Polosan, M. Bettinelli, T. Tsuboi, Phys. Stat. Sol. (c) 4 (2007) 1352.

[5] R.L. Remski, L.T. James, K.H. Gooen, B. Di Bartolo, A. Linz, IEEE J. Quantum Electron. QE-15 (1969) 214.

[6] E.P. ChiMis, C.S. Naiman, R.C. Folweiler, D.R. Gabbe, H.P. Jenssen, A. Linz, Appl. Phys. Lett. 19 (1971) 119.

[7] E.V. Boiko, V.F. Danilichev, N.N. Smirnov, V.V. Lazo, Proceedings, Conference on Lasers and Electro-Optics Europe (1994) 216.

[8] G. H. Dieke, Spectra and Energy Levels of Rare Earth Ions in Crystals, edited by H.M. Crosswhite and H. Crosswhite, Wiley Interscience Publishers, (New York, 1968).

[9] M.B. Seelbinder, J.C. Wright, Phys. Rev. B 20 (1979) 4308.

[10] E. Osiac, I. Sokolska, S. Kuck, J. Alloy Comp. 323-324 (2001) 283.

[11] I. Sokolsaka, S. Kuck, G. Dominiak-Dzik, M. Baba, J. Alloy Comp. 323-324 (2001) 273.

[12] J.P. Van Der Ziel, L.G. Van Uitert, Phys. Rev. 180 (1969) 343.

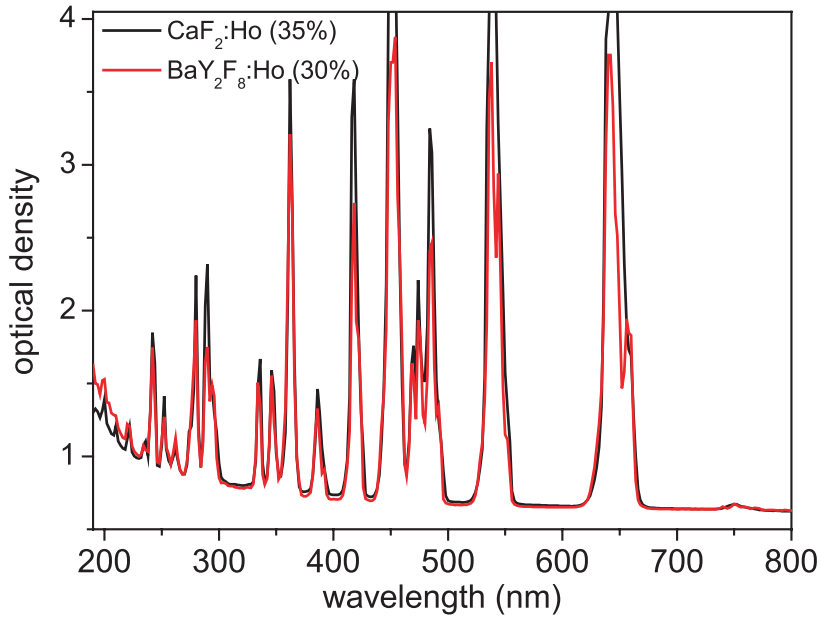

Fig. 1 Ultraviolet-visible absorption spectra of Ho^{3+} ions in 30% Ho^{3+}-doped BaY_2F_8 and 35% Ho^{3+}-doped CaF_2 crystals at room temperature.

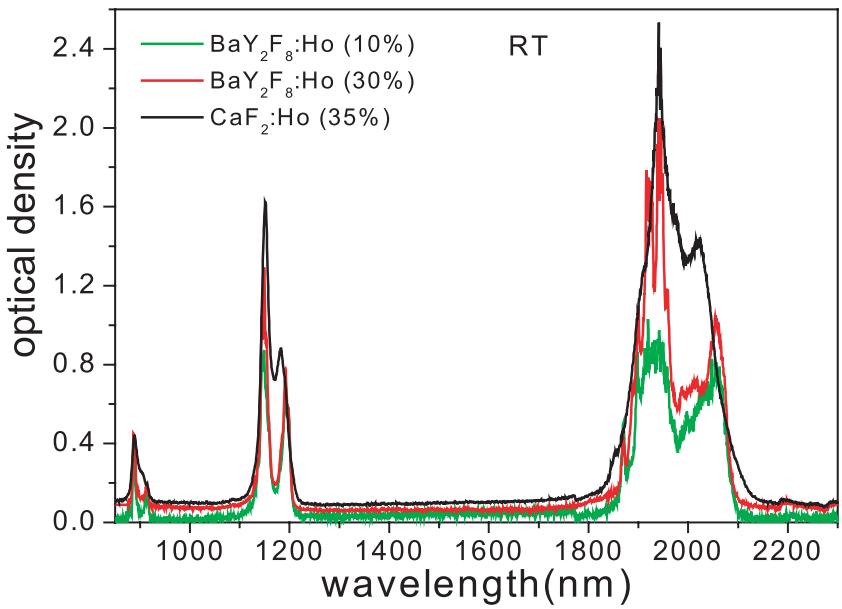

Fig. 2 Near-infrared absorption spectra of Ho^{3+} ions in 10% and 30% Ho^{3+}-doped BaY_2F_8 and 35% Ho^{3+}-doped CaF_2 crystals at room temperature.

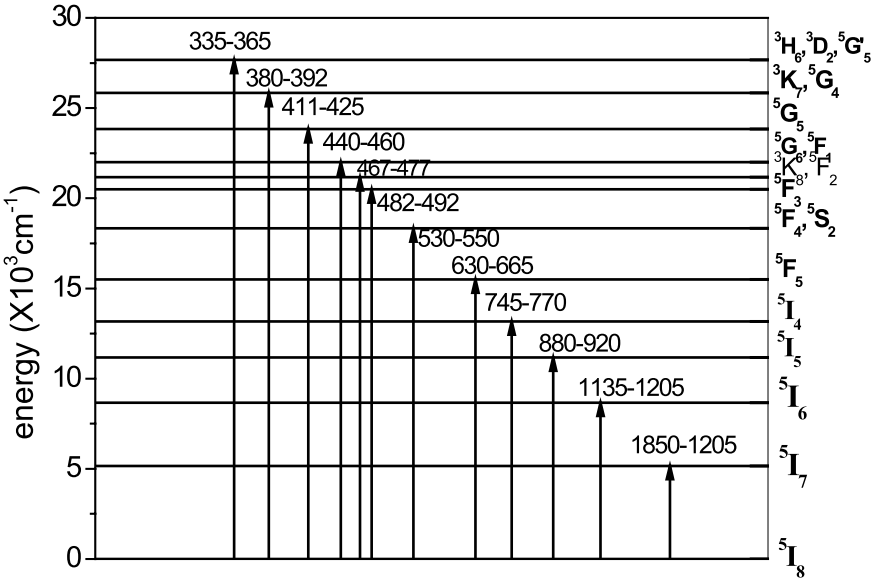

Fig.3 Level assignment for the absorption bands due to Ho^{3+} ion. The number such as 1850-1205 indicates the absorption band at 1850-1205 nm region.

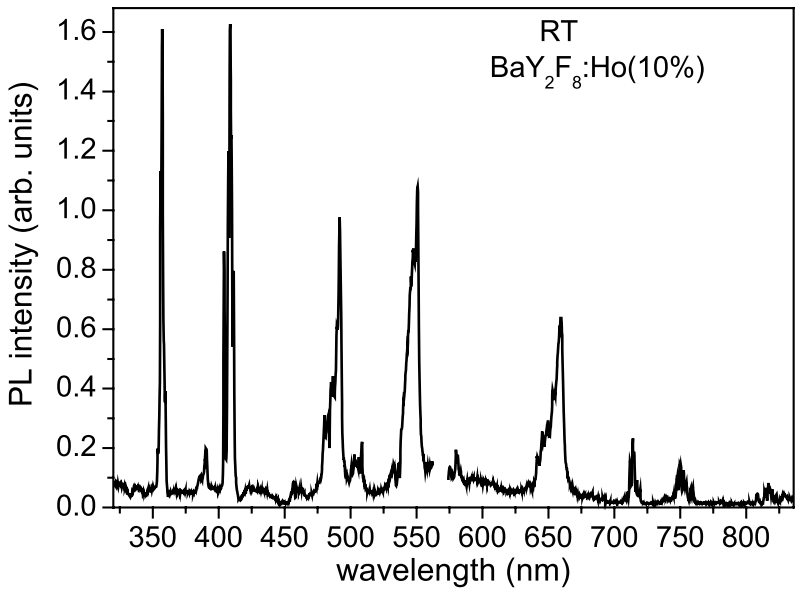

Fig.4 The PL spectrum of 10% Ho^{3+}-doped BaY_2F_8 crystal which was excited at 285 nm at room temperature. Spectrum in the range of 555-575 nm is deleted because of intense band due to the second harmonic of 285 nm excitation light.

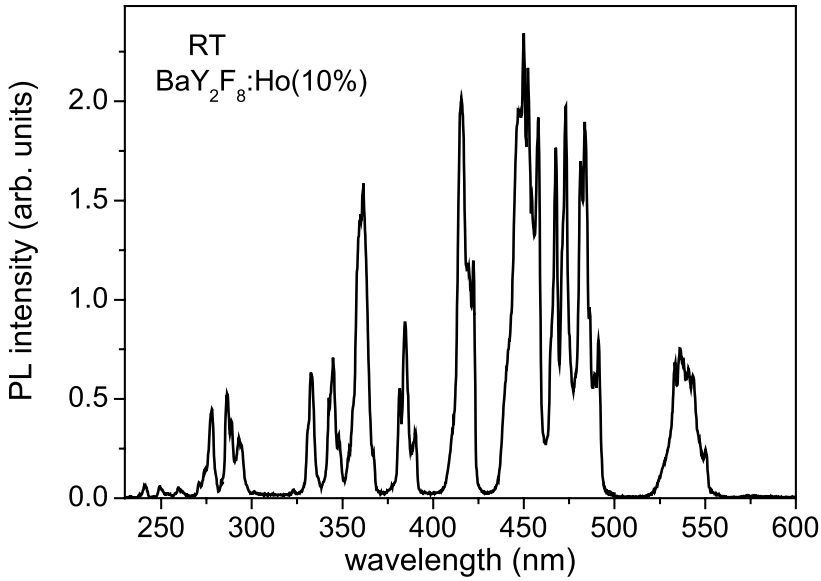

Fig.5 The PLE spectrum for 660 nm emission of 10% Ho^{3+}-doped BaY_2F_8 crystal at room temperature.

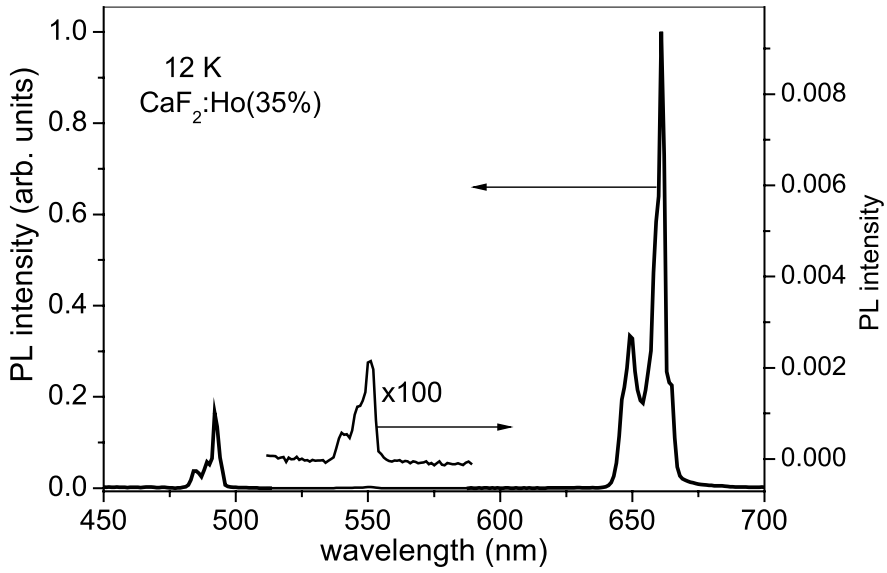

Fig.6 The PL spectra of 35% Ho^{3+}-doped CaF_2 crystal which was excited at 383 nm at 12 K. The band at about 550 nm is enlarged by 100 times.

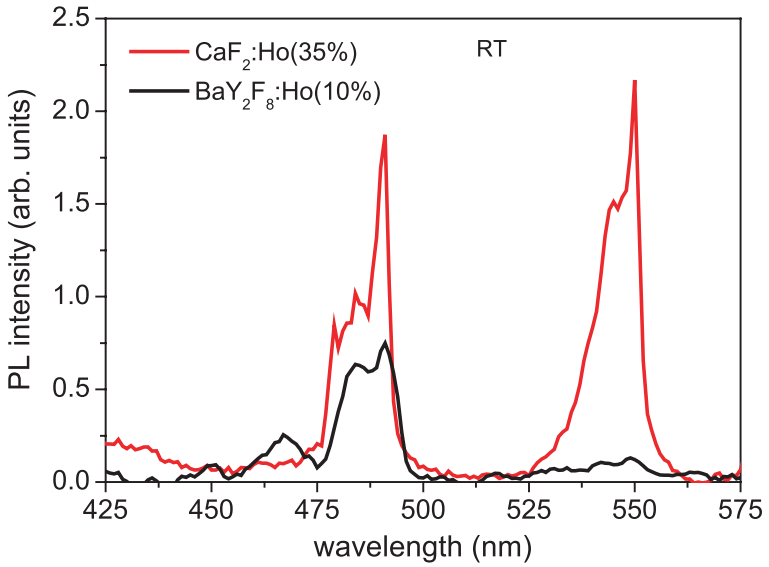

Fig.7 The PL spectra of 35% Ho^{3+}-doped CaF_2 and 10% Ho^{3+}-doped BaY_2F_8 crystals which were excited at 360 nm at room temperature.

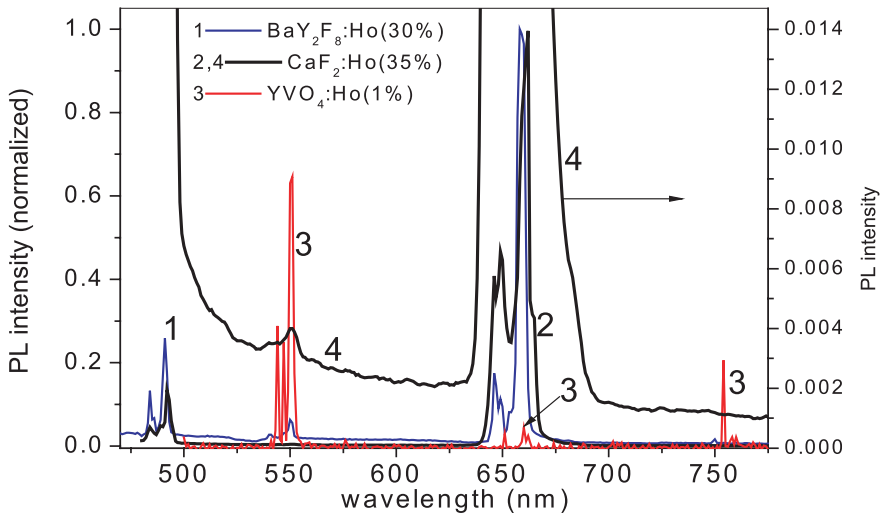

Fig.8 Visible PL spectra of 30% Ho^{3+}-doped BaY_2F_8, 35% Ho^{3+}-doped CaF_2 and 1% Ho^{3+}-doped YVO_4 crystals which were excited at 447 nm at 12 K.

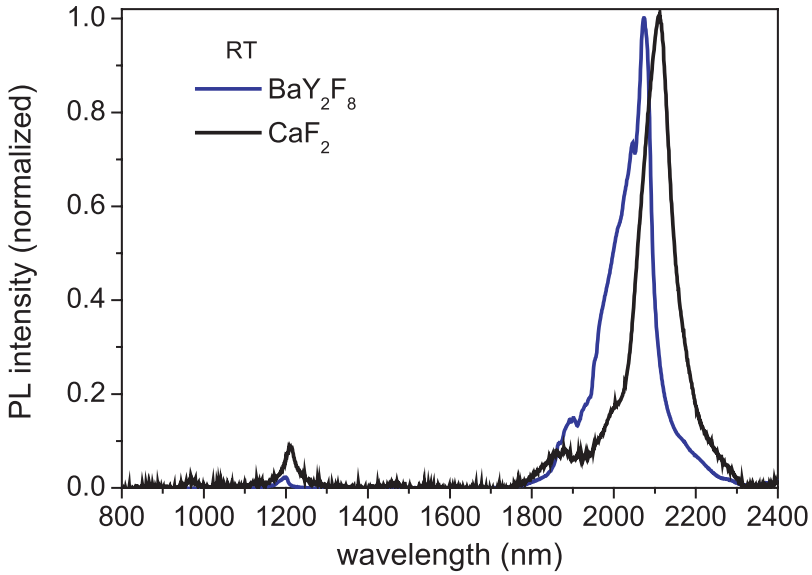

Fig.9 Near-infrared PL spectra of 30% Ho^{3+}-doped BaY_2F_8 and 35% Ho^{3+}-doped CaF_2 crystals which were excited at 360 nm at room temperature.

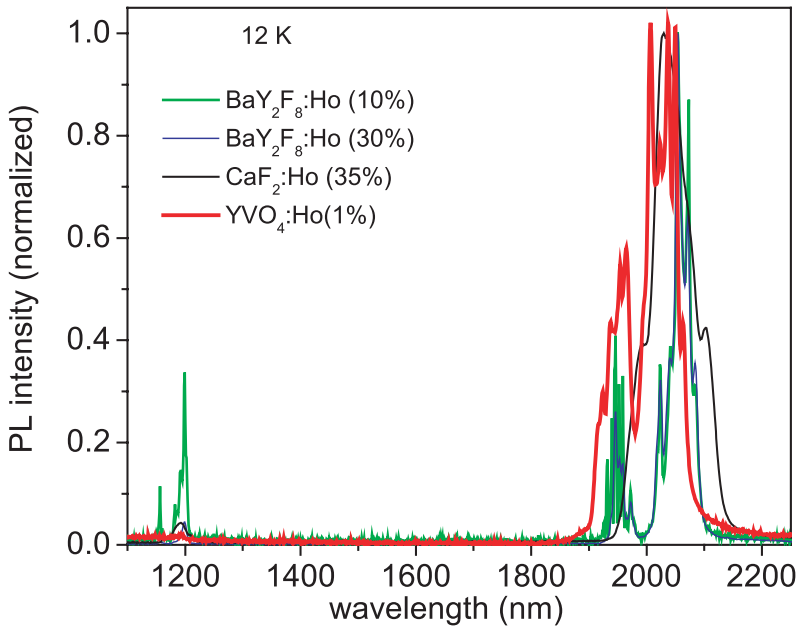

Fig.10 Near-infrared PL spectra of 10% and 30% Ho^{3+}-doped BaY_2F_8, 35% Ho^{3+}-doped CaF_2 and 1% Ho^{3+}-doped YVO_4 crystals which were excited at 447 nm at 12 K.

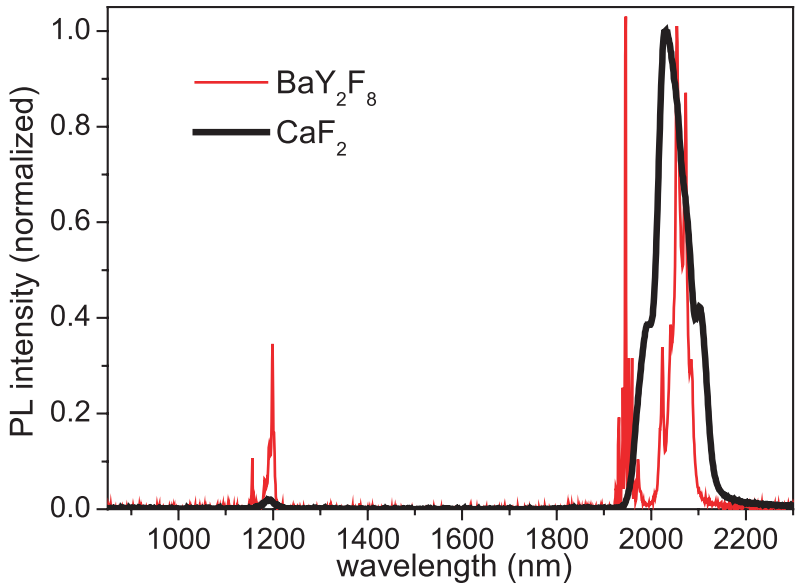

Fig. 11 Near-infrared PL spectra of 10% Ho^{3+}-doped BaY_2F_8 and 35% Ho^{3+}-doped CaF_2 crystals which were excited at 533 nm at 12 K.

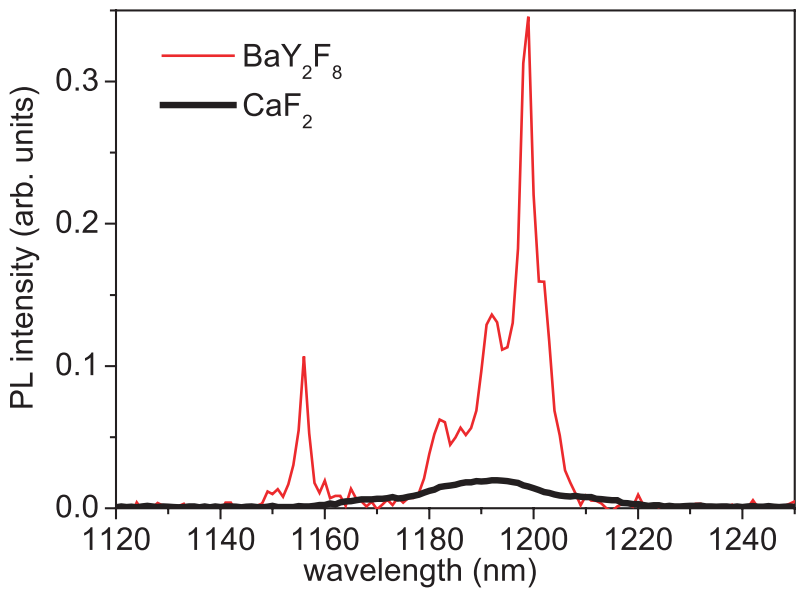

Fig. 12 Enlarged PL spectra, in the 1120-1250 nm range, of Fig. 11.

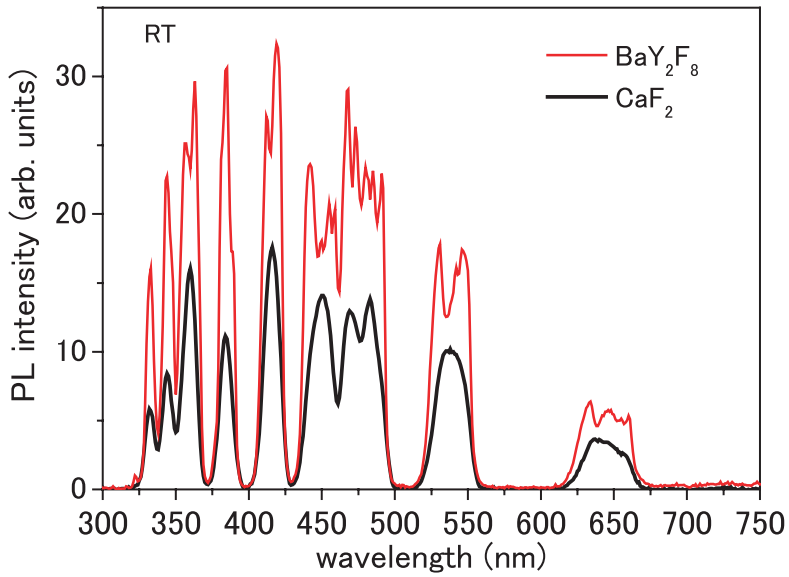

Fig.13 The PLE spectra for 2073 nm emission of 30% Ho^{3+}-doped BaY_2F_8 crystal and for 2110 nm emission of 35% Ho^{3+}-doped CaF_2 crystal at room temperature.

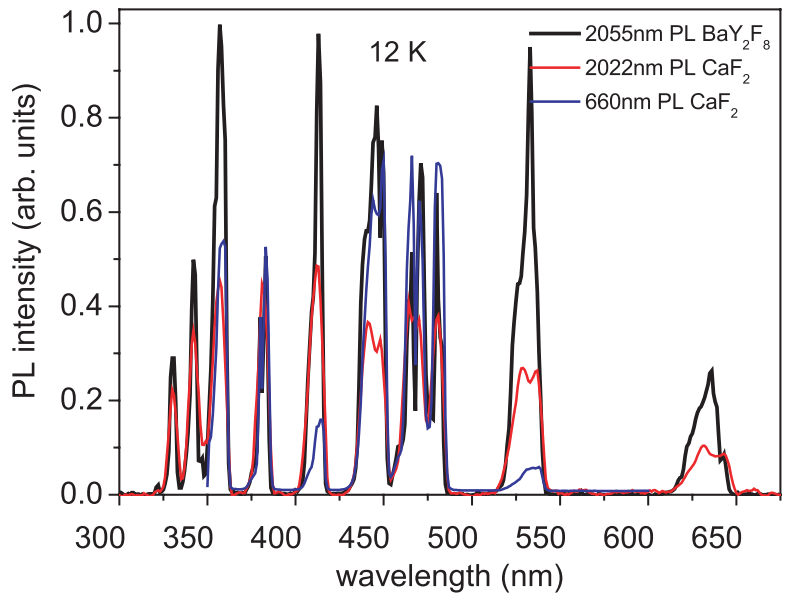

Fig.14 The PLE spectra for 2055 nm emission of 10% Ho^{3+}-doped BaY_2F_8 crystal, for 2022 nm emission of 35% Ho^{3+}-doped CaF_2 crystal and for 660 nm emission of 35% Ho^{3+}-doped CaF_2 crystal at room temperature.

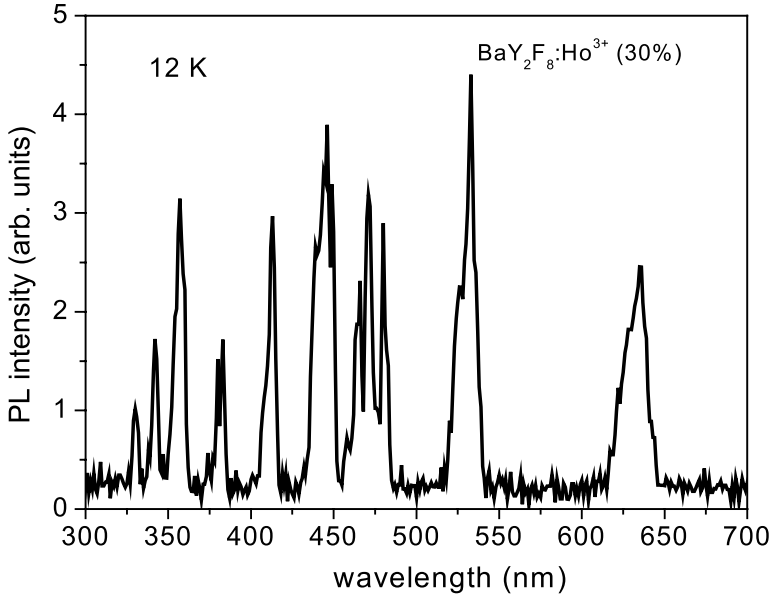

Fig.15 The PLE spectrum for 2100 nm emission of 30% Ho^{3+}-doped BaY_2F_8 crystal at 12 K.

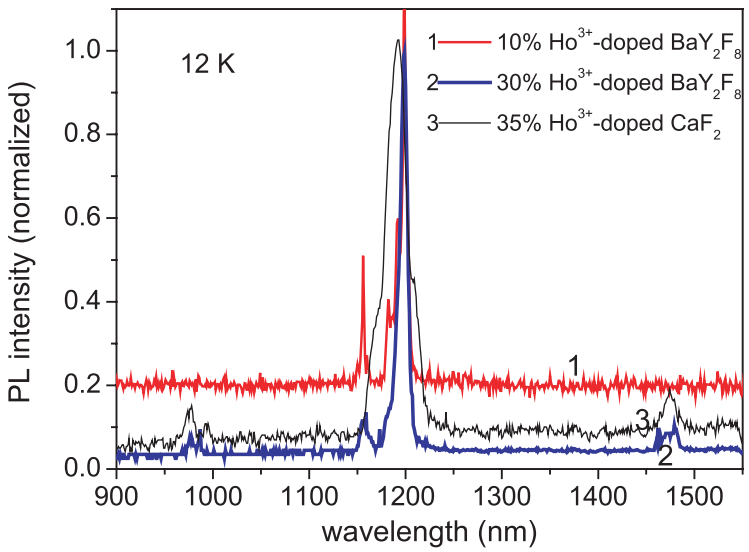

Fig.16 Near-infrared PL spectra of 10% and 30% Ho^{3+}-doped BaY_2F_8 and 35% Ho^{3+}-doped CaF_2 crystals which were excited at 447 nm at 12 K. Figure is normalized at 1190 nm PL peak.

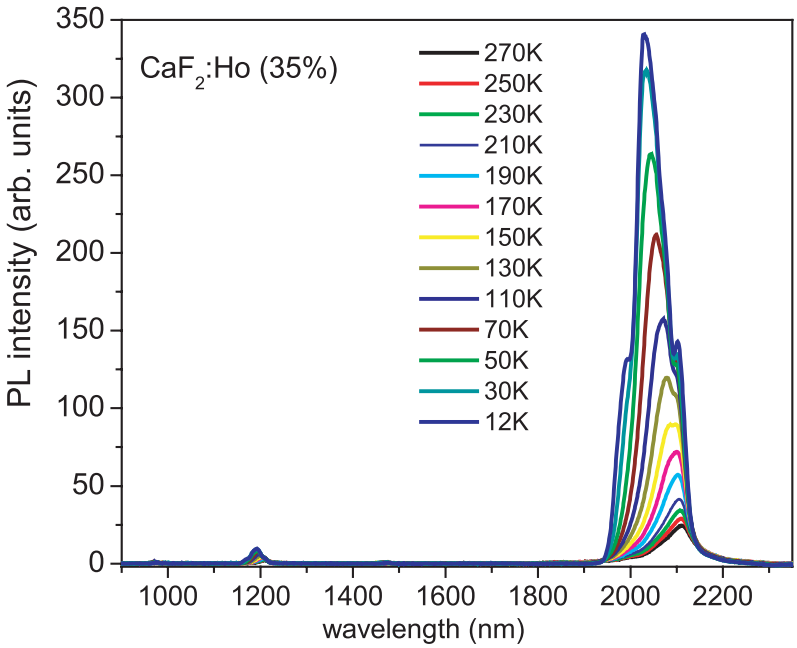

Fig.17 Temperature dependence of the near-infrared PL spectra of 35% Ho^{3+}-doped CaF_2 crystal which was excited at 360 nm.

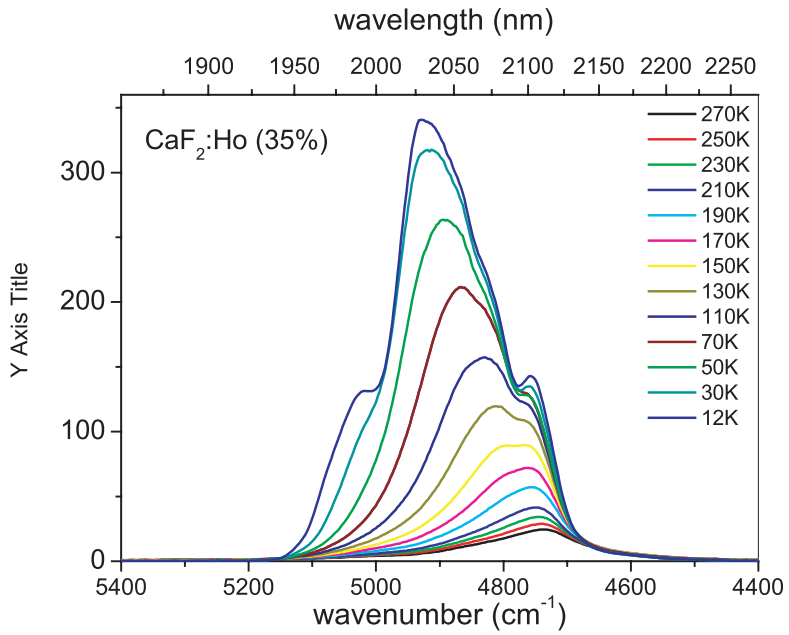

Fig.18 Temperature dependence of the 2040nm PL band, plotted against wavenumber in linear scale, of 35% Ho^{3+}-doped CaF_2 crystal which was excited at 360 nm.

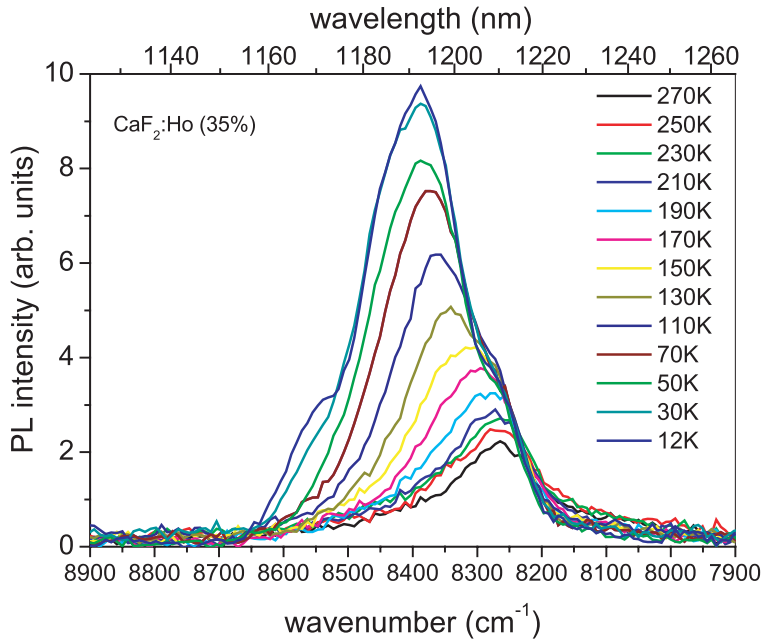

Fig.19 Temperature dependence of the 1190 nm PL band, plotted against wavenumber in linear scale, of 35% Ho^{3+}-doped CaF_2 crystal which was excited at 360 nm.

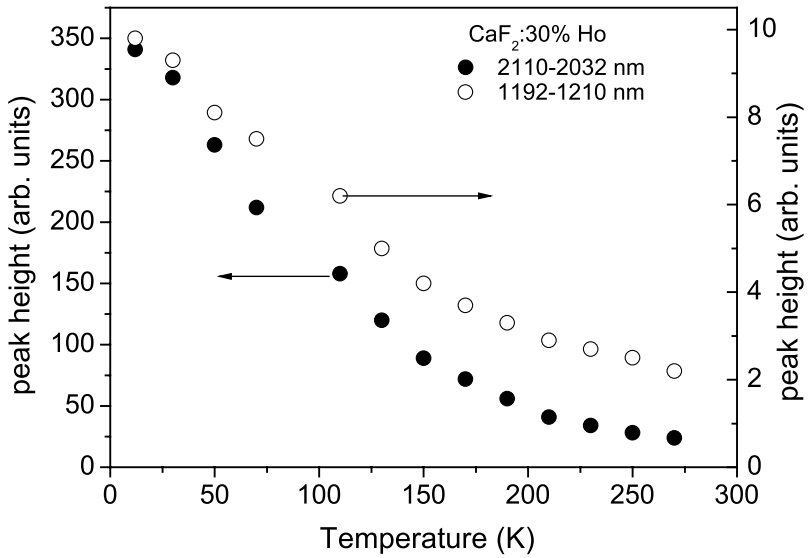

Fig.20 Temperature dependence of the peak height of the 2040 and 1190 nm PL bands in 35% Ho^{3+}-doped CaF_2 crystal which were excited at 360 nm.

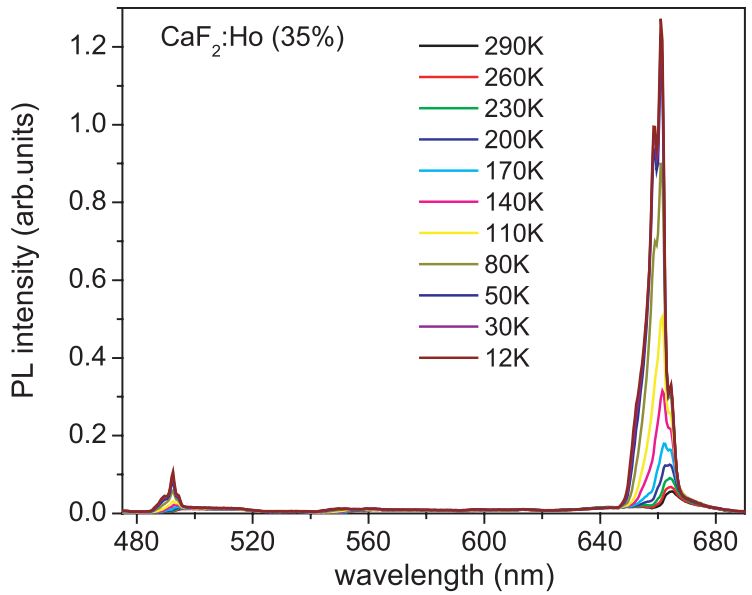

Fig.21 Temperature dependence of the visible PL spectra of 35% Ho^{3+}-doped CaF_2 crystal which was excited at 360 nm.

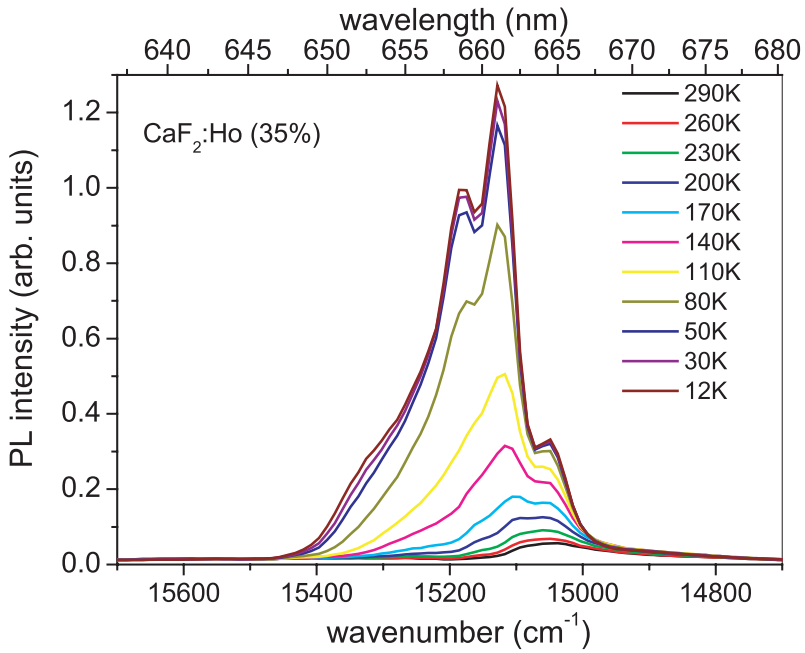

Fig.22 Temperature dependence of the 658 nm PL band, plotted against wavenumber in linear scale, of 35% Ho^{3+}-doped CaF_2 crystal which was excited at 360 nm.

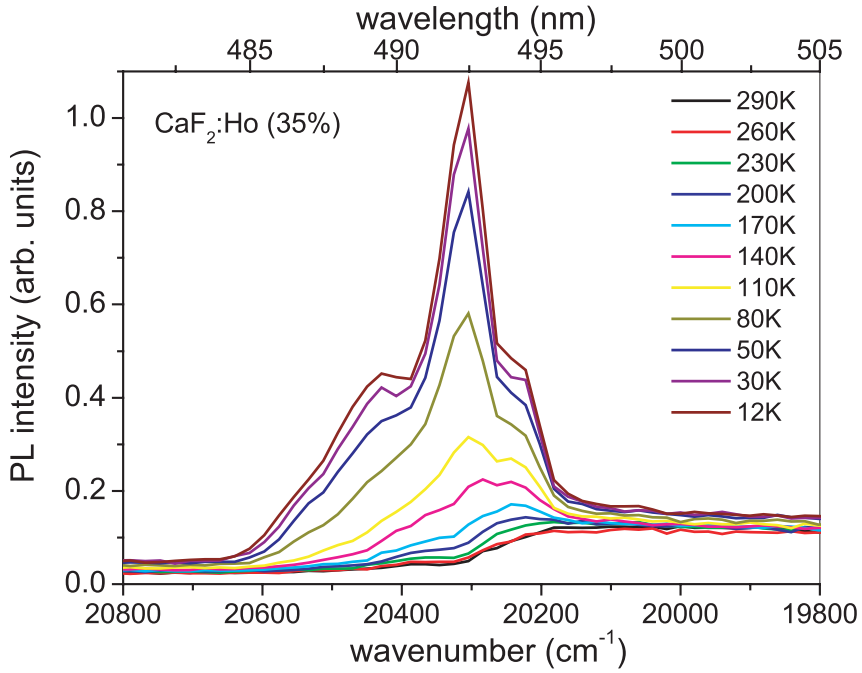

Fig.23 Temperature dependence of the 493 nm PL band, plotted against wavenumber in linear scale, of 35% Ho^{3+}-doped CaF_2 crystal which was excited at 360 nm.